Mon. Not. R. Astron. Soc. **299,** 777–788 (1998)

Mass functions of five distant northern open star clusters

Ram Sagar[1⋆] and W. K. Griffiths[2⋆]
[1] *Uttar Pradesh State Observatory, Manora Peak, Naini Tal–263129, India*
[2] *Department of Physics and Astronomy, The University of Leeds, Leeds LS2 9JT*

Accepted 1998 May 11. Received 1998 April 15; in original form 1997 May 9

ABSTRACT

We analyse *BVI* CCD data of five northern open star clusters in the Galaxy in order to determine their mass functions. The clusters are Berkeley 81, Berkeley 99, NGC 6603, NGC 7044 and NGC 7510. They are distant (≥ 3 kpc) and compact (radius $\leq$2.8 arcmin) objects. Except for NGC 7510 whose age is 10 Myr, all are intermediate-age and old star clusters with ages between 0.5 and 3.2 Gyr. The observed cluster luminosity function (LF) is corrected for both data incompleteness and field star contamination. Theoretical stellar evolutionary isochrones are used to convert LFs into mass functions (MFs). The MF slope becomes flatter if a correction for data incompleteness is not applied, while it becomes steeper if a correction for field star contamination is ignored; however, both corrections increase with decreasing stellar brightness.

In the mass range $\sim$1–14 $M_{\odot}$, the MF slope of NGC 7510 is 1.1 ± 0.2. As the cluster is not dynamically evolved, its present-day MF can be considered as the initial MF. It is not too different from the Salpeter value ($x = 1.35$). In a narrow mass range $\sim 0.6 - 2\ M_{\odot}$, the values of the MF slope in the four intermediate-age and old clusters range from 0.3 to 2.5 and differ significantly from each other. For Berkeley 99 and NGC 6603, the MF slopes are 1.4 ± 0.6 and 1.1 ± 0.4 respectively. They agree with the Salpeter value within the errors. However, significantly different values of MF slopes, 2.5 ± 0.2 and 0.3 ± 0.2, are found for Berkeley 81 and NGC 7044 respectively. We therefore conclude that the MF does vary among this cluster sample.

The effects of mass segregation are observed in all the four intermediate-age and old clusters; this segregation is most probably due to dynamical evolution, as the ages of the clusters are much longer than the corresponding dynamical relaxation times.

There is no obvious dependence of the MF slope on either Galactocentric distance or age of the well-studied Galactic open clusters. Except for some of the dynamically evolved older (age $\geq$50 Myr) clusters, the MF slopes of the clusters are not too different from the Salpeter value.

Key words: stars: luminosity function, mass function – open clusters and associations: general.

1 INTRODUCTION

The distribution of stellar mass at birth is defined as the initial mass function (IMF). Detailed knowledge of the IMF in different environments is crucial for studies that attempt to describe the spectral, photometric, and chemical evolution of integrated stellar systems, because mass is one of the primary parameters which dictate the evolution of stars. Knowledge of the IMF is also important for constraining star formation theories and for understanding the early evolution of star clusters, because it is a fossil record of the very complex process of star formation and provides an important link between the easily observable population of luminous stars in a stellar system and the fainter, but dynamically more important, low-mass stars. The IMF is one of the fundamental properties that must be explained by any complete theory of the star formation process (cf. Richtler 1994, and references therein).

A fundamental question in the theories of stellar and galactic evolution is whether the shape of the IMF is universal in time and space, or whether it depends on parameters like metallicity, age, environment, etc. In spite of many years of continued observations, the answers are still unknown (cf. Scalo 1986, 1998). In particular, the appropriate size-scale over which the star formation processes produce a frequency distribution of stellar masses exhibited by the field star IMF is not known. In this regard, open star clusters in our

⋆E-mail: sagar@upso.ernet.in (RS); w.k.griffiths@leeds.ac.uk (WKG)

Galaxy provide important laboratories for such study, since they present the smallest size-scales for making meaningful comparisons with the field star IMF. They also possess many favourable characteristics for IMF studies. Since each cluster contains an (almost) coeval set of stars at the same distance with the same metallicity, many of the most severe difficulties associated with determining the MF from field stars may be avoided, including complex corrections for stellar birth rates, lifetimes, and spatial variations. Therefore, in the simplest imaginable situation, the observed MF of a star cluster is equivalent to its IMF, and it can *in principle* be determined from the observed LF using theoretical stellar evolutionary models. *In reality* the situation is different, because the stellar MF of any star cluster changes with time due to stellar as well as dynamical evolutionary effects. The inherently small number of stars in open clusters results in large statistical uncertainties, and most open clusters are located in the Galactic plane and suffer extensive field star contamination.

An early and important study of the LFs of 20 star clusters was carried out by van den Bergh & Sher (1960). They found variations in the LFs, with an apparent turnover at fainter magnitudes, unlike that seen in the field star IMF. In recent years, luminosity and mass functions have been determined for a number of open clusters using homogeneous photoelectric or CCD data and reliable cluster membership (cf. Piskunov 1976; Sagar et al. 1986, 1988; Scalo 1986, 1998; Kjeldsen & Fransden 1991; Phelps & Janes 1993, and references therein). The average slope of the IMF seems to be not very different from the Salpeter (1955) value, but uncertainties are large and a few objects also showed significant variation from this average value.

Given the fact that only a few of the large number of Galactic star clusters have been used to study the IMF, it is clear that we are at the beginning in utilizing the potential offered by them. In the present work we derive MF slopes of five distant open star clusters, namely Berkeley 81, Berkeley 99, NGC 6603, NGC 7044 and NGC 7510, using *BVI* CCD data. Coordinates and other relevant information on these clusters are given in Table 1. The effects of data incompleteness and field star contamination corrections on the MF slopes of the clusters under study are analysed. The dependence of the MF slope on the cluster location and its age is also studied.

2 OBSERVATIONAL DATA

The *BVI* CCD data were obtained between July 21 and 24 1988 using an RCA SID 501 thinned back-illuminated CCD detector at the *f*/3.29 prime focus of the 2.3-m INT on La Palma. A detailed description of the observations and data reduction is given in our earlier papers (Sagar & Griffiths 1991, 1998, hereafter Papers I and II respectively). Briefly, one pixel of the 320×512 size CCD chip corresponds to 0.74 arcsec, and the entire chip covers a field of $\sim 4.0 \times 6.3$ arcmin^2 on the sky. The nights were of good photometric quality, with best and worst seeing $\sim$1.2 and 2.0 arcsec respectively. We imaged overlapping regions for all clusters.

The crowded field stellar photometric routine in DAOPHOT was used for the magnitude determination. These magnitudes were calibrated using nine Landolt (1983) photoelectric standards, covering a range in brightness ($10 < V < 12.75$) as well as in colour ($-0.19 < V - I < 1.41$). The photometric data have an uncertainty of $\sim$0.02 mag in the zero-points of B, V and I. This source of error is of negligible importance in determining the stellar LFs. The present CCD data agree very well with independent photoelectric observations of some stars in NGC 7510, and with CCD observations in NGC 6603 and 7044. However, some CCD observations show significant differences of $\sim$0.1 mag (cf. Papers I and II). The (X, Y) pixel coordinates, identification maps and *BVI* magnitudes of stars used in this work have been given in Paper I for NGC 7510, and in Paper II for Berkeley 81, Berkeley 99, NGC 6603 and NGC 7044. The stellar contents in Berkeley 81 and Berkeley 99 have been studied for the first time.

Table 1. Coordinates and other relevant information on the clusters under study. They are taken from the catalogue of Lyngå (1987). Distance, $E(V-I)$ and age for NGC 7510 are taken from Paper I, while those for Berkeley 81, Berkeley 99, NGC 6603 and NGC 7044 are taken from Paper II. For determining the Galactocentric distances to the clusters, a value of 8.8 kpc has been assumed for the Galactocentric distance of the Sun.

Cluster	Galactic coordinates				Distance	E(V-I)	Age
	l	b	R	z			
	(°)	(°)	(kpc)	(pc)	(kpc)	(mag)	(Myr)
NGC 6603	12.86	−1.32	6.3	−60	2.6	0.67	500
Berkeley 81	33.64	−2.51	6.5	−131	3.0	1.25	1000
NGC 7044	85.87	−4.13	9.1	−216	3.0	0.88	1600
NGC 7510	110.96	−0.05	10.4	−3	3.2	1.25	10
Berkeley 99	115.95	10.11	11.8	865	4.9	0.40	3200

3 CLUSTER LUMINOSITY FUNCTIONS

The LFs of star clusters and their corresponding field regions were determined from star counts of main-sequence (MS), generally in bin widths of 1 mag in V. The main factors which limit the precise determination of LFs from the present observations are the limited knowledge of accurate cluster parameters, data incompleteness and field star contamination. Their estimation and treatment in the present analysis are described in the following subsections.

3.1 Distance, reddening and age of the clusters

The cluster parameters listed in Table 1 are derived from deep ($V \sim 22$ mag) CCD observations carried out earlier by us (see Papers I and II). The accuracy of distance estimates is $\sim$15 per cent, while that of age determination is about 20 per cent. An accurate knowledge of extinction across the cluster face is also required. Presence of non-uniform (differential) interstellar extinction has generally been noticed in Galactic open clusters younger than 10^8 yr (cf. Sagar 1987, and references therein). The extent of differential extinction decreases with cluster age, as the interstellar matter responsible for it is either consumed in star formation or blown away by the radiation pressure of hot stars present in the clusters. The clusters under study are compact (radius $\leq$2.8 arcmin) and older than 0.5 Gyr, except NGC 7510 which is only 10 Myr old, but all are located $\geq$3 kpc away from us. As the presence of differential extinction across the cluster face will widen the cluster MS, it is worth knowing whether it is present in the clusters under study or not and, if present, then its extent. Investigations in our Paper I indicate that the interstellar extinction is non-uniform across the face of the cluster NGC 7510, with the value of colour excess, $E(B-V)$, ranging from 1.0 to 1.3 mag. In order to see whether interstellar extinction across the face of other clusters under study is uniform or not, we divided the observed area of each cluster into four equal rectangular regions and estimated the mean location of the cluster sequence and scatter around it in the $V, (B-V)$ and $V, (V-I)$ diagrams of each region. Almost the same mean location of the cluster sequence and the scatter around it are observed in the

Table 2. Pixel coordinates of the field and the cluster regions. One pixel corresponds to 0.74 arcsec on the sky. The (X_c, Y_c) are coordinates of the cluster centre. The cluster region is an area within a radius (R) of the cluster. The area of the cluster region is AR times the area of the field region.

Cluster	X_c (pixel)	Y_c (pixel)	R (pixel)	Field region (pixel)	AR
Berkeley 81	180	385	220	$X = 0$ to 510; $Y = 0$ to 150	1.20
Berkeley 99	300	250	230	$X = -150$ to 0; $Y = 160$ to 480 and $X = 0$ to 50; $Y = 50$ to 480 and $X = 0$ to 510; $Y = 0$ to 50	1.72
NGC 6603	380	200	230	$X = 0$ to 100; $Y = 0$ to 320 and $X = 650$ to 720; $Y = 0$ to 320	2.45
NGC 7044	110	230	180	$X = 0$ to 510; $Y = 450$ to 510 and $X = 350$ to 510; $Y = 0$ to 510	0.91
NGC 7510	230	245	200	$X = 0$ to 490; $Y = 0$ to 520 and R$\geq$ 250	2.10

colour–magnitude diagrams of different regions of each cluster. This indicates the presence of uniform extinction in the regions of clusters older than 500 Myr in our sample, and thus supports our earlier findings (cf. Sagar 1987).

In the light of the above discussion, constant values of $E(V-I)$ for the clusters given in Table 1 have been used in our further analysis, and the width of the MS observed in our Papers I and II has been used to define the cluster MS region. In the case of NGC 7510, additional MS widening introduced due to the presence of differential extinction has also been taken into account in the analysis.

3.2 Radius and centre of the clusters

The radial variation of stellar surface density (ρ) has been used to estimate cluster radius. For this, it is necessary to fix the cluster centre. We have derived it iteratively by calculating average X and Y positions of stars within 100 pixels from an eye estimated centre, until it converged to a constant value. The (X_c, Y_c) pixel values estimated in this way are listed in Table 2 along with the cluster radius, R. An uncertainty of a few pixels is expected in locating the cluster centre, while radius determinations are better than a few arcseconds. For Berkeley 81, Berkeley 99, NGC 6603 and NGC 7044, they are determined in our Paper II, while for NGC 7510, the analysis has been carried out below. The variation of $\log(\rho)$ with R is shown in Fig. 1 for NGC 7510. The profile given by King (1962) fits the observed data points satisfactorily. This analysis indicates that cluster radius is $\sim$200 pixel. The radius of the clusters under study thus ranges from $\sim$2.2 to 2.8 arcmin.

3.3 Cluster and field regions

We have generally observed a $\sim 6 \times 8$ arcmin^2 field centred around the cluster. The circular area within radius R from the cluster centre is considered as the cluster region. The objects under study are compact, with $R \leq 2.8$ arcmin, and rich in stellar content. So we may choose regions which are located beyond a cluster radius for estimating field star contamination in the cluster. The (X, Y) pixel coordinates of field regions selected in this way are listed in Table 2. The $V, (V-I)$ diagrams for both cluster and field regions of NGC 6603 are shown in Fig. 2. A comparison of angular separation between cluster and field regions with the value of cluster R indicates that the mean radial distance of the field regions is $\sim 1.4\,R$ from the cluster. The field regions are thus located close to the clusters. In order to see whether this has affected the determination of MS field star contamination significantly or not, we compared present NGC 6603 MS field star densities with those given by Bertelli et al. (1995) for a region located north of the cluster NGC 6603 at a radial distance of 15 arcmin ($> 5R$) and covering an area of 10 arcmin^2. The field region we used has an area of 8.3 arcmin^2. Fig. 3 compares the two observed MS stellar distributions. The number of MS stars observed by Bertelli et al. (1995) has been corrected for the difference in area. We have not applied data incompleteness corrections, as they are similar in both CCD observations. The observed MS stellar distributions in the two field regions located at different radial distances generally agree within statistical fluctuations (see Fig. 3). We therefore conclude that although the MS field star contamination determination is based on an area located not very far from the cluster, it does not include a significant number of MS cluster members, at least in the case of NGC 6603. However, we have analysed the effect of this on the MF slope of the clusters under study in Section 4.3.

Except in the case of NGC 7044, the area of the chosen field region is less than that of the cluster region (see Table 2). However, it is large enough to derive a statistically significant LF for the field region (see Table 5).

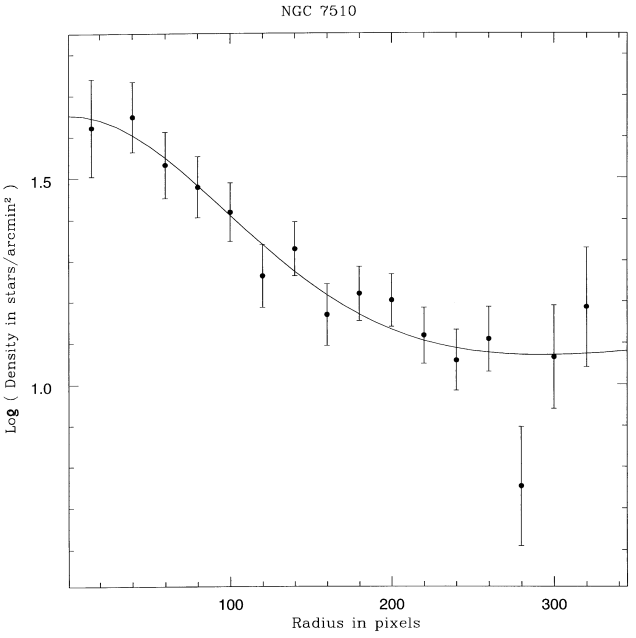

Figure 1. The variation of stellar surface density with radius for NGC 7510. The lengths of the bars represent errors due to sampling statistics. The curve shows a least-squares fit of the King (1962) profile.

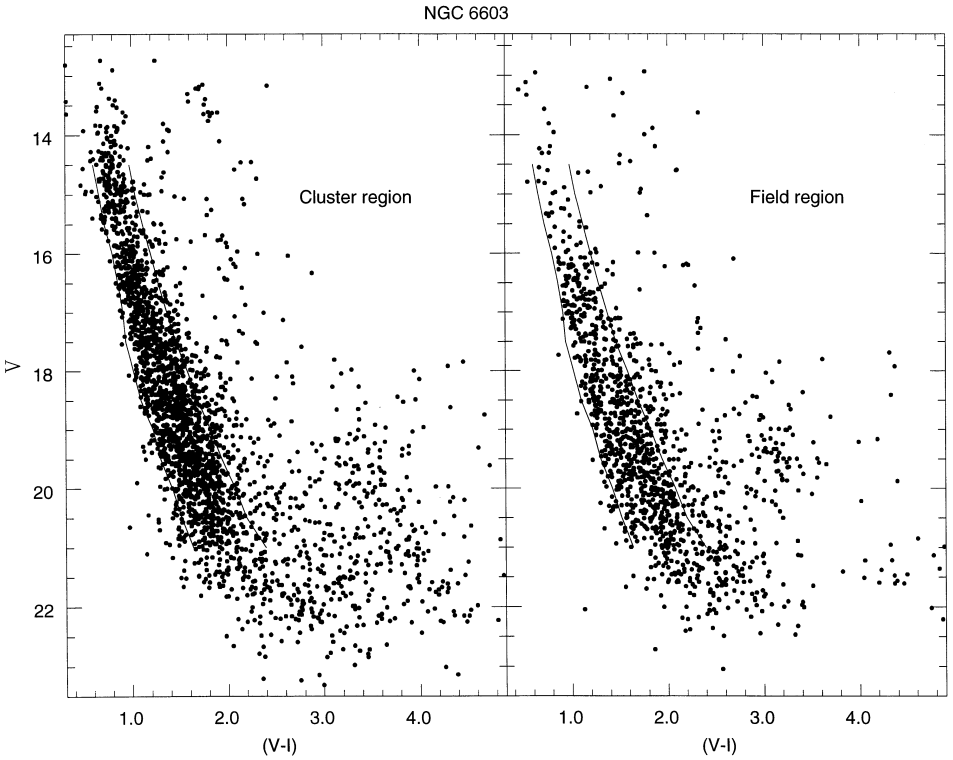

Figure 2. $V, (V - I)$ diagrams for stars of the NGC 6603 cluster and field regions. The slanted lines envelope the main-sequence stars and thus separate them from others.

3.4 Determination of photometric completeness

The method for determining the completeness factor, CF, of the stellar photometric data on the CCD frames using the DAOPHOT software package has been discussed by several authors (see, e.g., Stetson 1987, Mateo 1988 and Sagar & Richtler 1991, and references therein). We inserted a total of 21 500 artificial stars into 10 frames taken in V and I bands. The brightness distribution of the inserted stars as well as the number of times they were inserted into a data frame are given in Table 3. The luminosity distribution of the artificial stars has been chosen in such a way that more stars are inserted into the fainter magnitude bins, because only a small fraction of them will be recovered during photometric reduction. Also, only a limited number (~10–15 per cent of the number of originally detected stars) are inserted at one time, so that the crowding characteristics of the original data frame remain almost unchanged. Thus, to have satisfactory number statistics for the determination of CF, 10 independent sets of artificial stars are inserted into a given data frame.

3.5 Data incompleteness and field star contamination corrections

The LF, defined as the variation in stellar counts per unit magnitude range, can in principle be derived from frames in one wavelength band only. Although on a single frame the completeness factors can easily be determined, since the values of CF as a function of brightness and crowding can be empirically determined, it is not possible to distinguish MS stars from evolved red giants and other non-MS stars. The latter play an important role in the construction of LFs for star clusters which are superimposed on fields composed

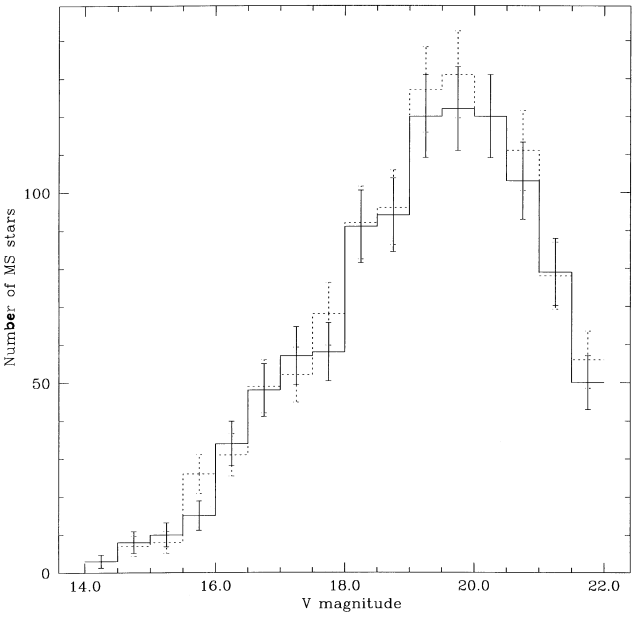

Figure 3. Comparison of main-sequence field star distributions. The frequency distribution derived from present data is shown by the solid line histogram while that given by Bertelli et al. (1995) is shown by the dotted histogram.

Table 3. Details of artificial star add experiments. The N_m, N_i and N_f are respectively the number of stars measured in original CCD frames, the number of stars inserted, and the number of artificial star frames generated from a given original CCD frame. The number of stars added to each frame is simply $N_i \Sigma N_f$. Δm is the magnitude range of artificial stars added to the frame.

Region	Filter	N_m	N_i	Δm	N_f
NGC 6603	V	2700	300	18.23−24.23	2
				19.23−24.23	1
				20.23−24.23	2
				21.23−24.23	2
				22.23−24.23	3
	I	4010	400	17.10−23.10	2
				18.10−23.10	1
				19.10−23.10	2
				20.10−23.10	2
				21.10−23.10	3
NGC 7044	V	1600	160	15.53−23.53	2
				16.53−23.53	1
				17.53−23.53	1
				18.53−23.53	2
				19.53−23.53	2
				20.53−23.53	2
	I	2030	200	14.01−22.01	2
				15.01−22.01	1
				16.01−22.01	1
				17.01−22.01	2
				18.01−22.01	2
				19.01−22.01	2
NGC 7510	V	580	60	15.72−21.72	2
				16.72−21.72	2
				17.72−21.72	2
				18.72−21.72	2
				19.72−21.72	2
	I	1300	130	15.46−21.46	2
				16.46−21.46	2
				17.46−21.46	2
				18.46−21.46	2
				19.46−21.46	2
Berkeley 81	V	2770	300	17.50−23.50	2
				18.50−23.50	2
				19.50−23.50	2
				20.50−23.50	2
				21.50−23.50	2
	I	3840	400	16.02−22.02	2
				17.02−22.02	2
				18.02−22.02	2
				19.02−22.02	2
				20.02−22.02	2
Berkeley 99	V	720	100	17.69−23.69	2
				18.69−23.69	2
				19.69−23.69	2
				20.69−23.69	2
				21.69−23.69	2
	I	900	100	16.34−22.34	2
				17.34−22.34	2
				18.34−22.34	2
				19.34−22.34	2
				20.34−22.34	2

Table 4. Variation of the completeness factor with MS brightness in both cluster and field regions. The CFB denotes the completeness derived using stars recovered in both V and I passbands; the CFP represents the product completeness factor of the pair derived from Mateo (1988) method, while CFM denotes the minimum completeness factor of the pair determined using the Sagar & Richtler (1991) technique.

Cluster	V mag of MS	Cluster region			Field region		
		CFB	CFM	CFP	CFB	CFM	CFP
Berkeley 81	16.75	1.00	1.00	1.00	1.00	1.00	1.00
	17.25	0.96	0.96	0.92	1.00	0.99	0.98
	17.75	0.95	0.93	0.86	1.00	0.98	0.96
	18.25	0.89	0.91	0.83	0.96	0.97	0.94
	18.75	0.87	0.90	0.81	0.93	0.95	0.90
	19.25	0.85	0.88	0.77	0.88	0.93	0.86
	19.75	0.81	0.83	0.71	0.86	0.91	0.83
	20.25	0.75	0.75	0.61	0.78	0.85	0.72
	20.75	0.66	0.72	0.52	0.75	0.76	0.58
	21.25	0.57	0.65	0.42	0.66	0.68	0.44
	21.75	0.47	0.58	0.34	0.60	0.61	0.37
	22.25	0.35	0.45	0.27	0.45	0.56	0.31
Berkeley 99	16.75	1.00	1.00	1.00	1.00	1.00	1.00
	17.25	1.00	1.00	1.00	1.00	1.00	1.00
	17.75	0.97	1.00	1.00	1.00	1.00	1.00
	18.25	0.92	0.95	0.95	1.00	1.00	1.00
	18.75	0.88	0.92	0.91	1.00	1.00	1.00
	19.25	0.85	0.86	0.84	0.96	0.96	0.96
	19.75	0.82	0.84	0.81	0.90	0.92	0.92
	20.25	0.80	0.80	0.77	0.86	0.88	0.88
	20.75	0.76	0.77	0.73	0.82	0.84	0.83
	21.25	0.74	0.75	0.70	0.80	0.81	0.79
	21.75	0.72	0.73	0.66	0.79	0.79	0.75
	22.25	0.70	0.70	0.61	0.75	0.75	0.68
	22.75	0.65	0.65	0.54	0.72	0.72	0.63
	23.25	0.60	0.60	0.36	0.60	0.65	0.42
NGC 6603	14.75	1.00	1.00	1.00	1.00	1.00	1.00
	15.25	1.00	1.00	1.00	1.00	1.00	1.00
	15.75	0.99	0.99	0.98	1.00	1.00	1.00
	16.25	0.97	0.99	0.98	1.00	1.00	1.00
	16.75	0.95	0.98	0.96	0.98	0.99	0.98
	17.25	0.93	0.95	0.90	0.97	0.98	0.96
	17.75	0.91	0.92	0.84	0.96	0.96	0.92
	18.25	0.83	0.85	0.72	0.92	0.93	0.86
	18.75	0.77	0.78	0.61	0.88	0.88	0.77
	19.25	0.71	0.71	0.50	0.81	0.82	0.67
	19.75	0.63	0.63	0.40	0.75	0.74	0.55
	20.25	0.59	0.56	0.31	0.70	0.65	0.42
	20.75	0.50	0.49	0.24	0.55	0.55	0.30
	21.25	0.40	0.38	0.14	0.50	0.45	0.20
NGC 7044	16.75	0.96	0.98	0.98	1.00	1.00	1.00
	17.25	0.90	0.92	0.91	0.99	1.00	1.00
	17.75	0.85	0.88	0.85	0.97	0.98	0.98
	18.25	0.83	0.81	0.78	0.92	0.94	0.93
	18.75	0.80	0.76	0.70	0.90	0.90	0.88
	19.25	0.76	0.74	0.65	0.88	0.87	0.83
	19.75	0.74	0.73	0.63	0.84	0.84	0.80
	20.25	0.70	0.71	0.60	0.81	0.82	0.76
	20.75	0.65	0.69	0.56	0.80	0.79	0.70
	21.25	0.62	0.67	0.51	0.76	0.77	0.66
	21.75	0.60	0.65	0.46	0.72	0.75	0.63
	22.25	0.57	0.61	0.39	0.70	0.72	0.58
	22.75	0.56	0.58	0.33	0.67	0.66	0.50
NGC 7510	14.75	1.00	1.00	1.00	1.00	1.00	1.00
	15.25	1.00	1.00	1.00	1.00	1.00	1.00
	15.75	1.00	1.00	1.00	1.00	1.00	1.00
	16.25	1.00	1.00	1.00	1.00	1.00	1.00
	16.75	1.00	1.00	1.00	1.00	1.00	1.00
	17.25	0.98	0.99	0.98	1.00	1.00	1.00
	17.75	0.97	0.96	0.92	1.00	0.98	0.96
	18.25	0.96	0.94	0.88	0.99	0.96	0.92
	18.75	0.94	0.93	0.86	0.96	0.95	0.90
	19.25	0.92	0.91	0.83	0.93	0.92	0.85
	19.75	0.90	0.90	0.81	0.92	0.91	0.83
	20.25	0.85	0.88	0.77	0.90	0.89	0.79
	20.75	0.80	0.84	0.71	0.85	0.86	0.74
	21.25	0.74	0.72	0.52	0.80	0.84	0.71

of a significantly different mix of stellar populations. Two colours, such as B and V or V and I, are required for their identification. It is therefore required to construct the MS LF either from a $V,(B-V)$ diagram or from a $V,(V-I)$ diagram instead of from a single B or V or I band. We preferred the $V,(V-I)$ diagram over the $V,(B-V)$ diagram, as it is generally deeper by at least by a magnitude. The MS stars have been isolated from others by drawing demarcation lines in the $V,(V-I)$ diagram (see Fig. 2). The main disadvantage of using two colours for the construction of the LF is that the process of matching the star image in both colours introduces further incompleteness, the treatment of which is by no means simple. Mateo (1988), for instance, assumes that the star counts in the two bands are independent, and adopts a completeness

factor, CFP, as the product of the CF values of the two frames. In contrast, Sagar & Richtler (1991) adopt CFM, the *minimum* value of the completeness factors of the pair, to correct the star counts. They argue that the two frames are not independent, and that the multiplicative assumption of Mateo (1988) could not be justified. The differences in these approaches are insignificant for the values of CF $\geq$0.95 in both passbands. However, they become progressively more pronounced for the decreasing values of CF. Mateo (1993) argues that the two methods represent the extremes possible in determining the data completeness. The Sagar & Richtler method assumes that a star counted in one colour is sure to be counted in the other colour – likewise for stars that are missed. On the other hand, the Mateo (1988) prescription assumes that the counts are perfectly uncorrelated. The values of CF determined by Sagar & Richtler are therefore likely to be underestimated for faint stars, while those by Mateo (1988) are over-estimated. To test the ability of these techniques to recover a known LF, Banks (1994) and Banks, Dodd & Sullivan (1995) performed numerical simulations and quantified the effects. They found that the product method of Mateo (1988) increasingly over-estimates the incompleteness correction as the magnitude is increased. The method suggested by Sagar & Richtler recovered the actual LF better, with a mean error of $\sim$3 per cent, although near the observational limit of the frames the technique underestimates the value of CF, since the assumption of the method fails there. They therefore used the Sagar & Richtler method for the bulk of their calculations, except when the value of CF fell below 50 per cent, which Stetson (1991) defines as the limiting magnitude of a CCD frame.

In fact, there is no need to decide how to combine the V and I completeness factors, if one determines the CF values along the MS in the $V,(V-I)$ diagram. We therefore added artificial stars to both V and I images simultaneously, in such a way that they have similar geometrical locations but differ in V and I brightness according to $(V-I)$ colours of the MS stars. Thus the same number of artificial stars were added to both V and I images by taking care of the photometric offsets and the coordinate shifts between the images. Table 3 shows the luminosity distribution of artificial stars added in the V band. The stars recovered in both V and I photometric data reduction have been used to determine the data completeness factor, CFB. The values obtained in this way are listed in Table 4 along with the values of CFM and CFP. They are determined for the MS of both cluster and field regions as a function of brightness. As expected, the data completeness factor becomes smaller with decreasing brightness and increasing stellar crowding. The uncertainties in the values are $\sim$0.03 and 0.04 for the field and cluster regions respectively. The values of CFB are compared with those of CFM and CFP in Fig. 4. The CFB values agree very well with the values of CFM, but differ significantly from the values of CFP at fainter brightnesses.

In the light of the above discussion, we have used the CFB values for the completeness factors in the present work, but we discuss the effects of other completeness factors on the MF slope.

The MS LF of both cluster and field regions has been determined from their $V,(V-I)$ diagrams. The star counts have been made either in 0.5- or 1.0-mag bins in V of the stars lying between the demarcation lines, as shown in Fig. 2 for NGC 6603. The brighter magnitude limit of the LF has been decided from the stellar evolutionary effects, while the fainter one has been decided from the data completeness limit, i.e., the brightness level where the value of CF becomes $\sim$50 per cent. The width of the magnitude bins has been chosen in such a way that statistically significant numbers of stars are present in all LF bins of both cluster and field regions. The results of the LF analysis are given in Table 5. The field star contamination generally increases with decreasing brightness.

Sagar & Richtler (1991) and Banks et al. (1995) have studied the

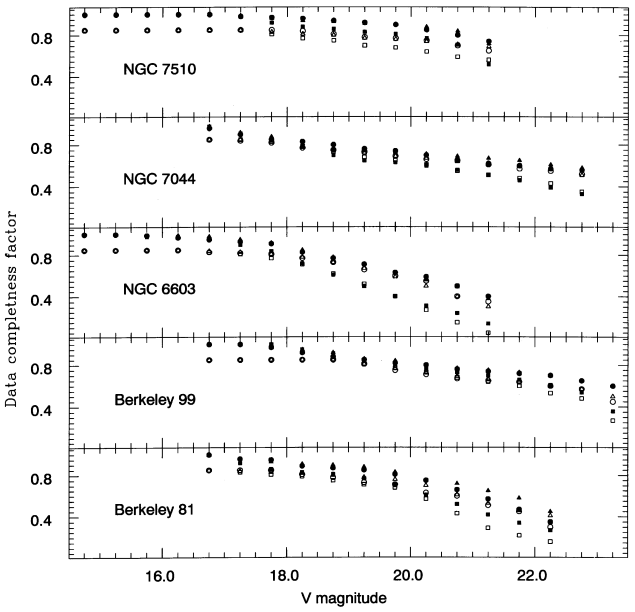

Figure 4. Comparison of data completeness factors. Filled circles, triangles and squares denote the CFB, CFM and CFP values for the cluster region, while the corresponding open symbols represent the same values for the field region. In order to present the points clearly, the values for field regions are offset by -0.15.

Table 5. Luminosity functions for the programme clusters. *NC* and *NF* denote star counts in V-magnitude bins derived from the main-sequence present in the $V,(V-I)$ diagrams of cluster and field regions respectively. Depending upon the corrections of field star contamination and/or data incompleteness, *NC* yields *N1*, *N2*, *N3*, *N4* and *N5* (see Section 3.5).

Cluster	Range in V mag	NC	NF	N1	N2	N3	N4	N5
Berkeley 81	17.0– 18.0	54	22	30.1	30.3	27.8	56.5	57.1
	18.0–19.0	101	46	56.8	54.5	36.0	115.0	111.8
	19.0–20.0	175	107	64.7	66.9	46.9	212.4	206.6
	20.0–21.0	297	211	94.9	88.0	44.3	426.2	405.3
	21.0–21.5	340	192	69.5	39.4	19.0	300.0	263.1
Berkeley 99	17.5–18.5	54	21	20.7	19.0	17.9	56.8	55.1
	18.5–19.5	64	16	46.3	44.4	36.5	74.2	72.3
	19.5–20.5	59	25	24.8	23.7	16.0	72.7	71.7
	20.5–21.5	62	23	35.8	33.8	22.4	84.6	81.7
	21.5–22.5	49	8	50.9	50.3	35.2	68.8	68.2
	22.5–23.5	52	11	55.0	55.9	32.9	83.3	83.3
NGC 6603	14.5–15.5	108	14	73.7	73.7	73.7	108.0	108.0
	15.5–16.5	133	23	79.8	78.1	77.3	136.0	134.3
	16.5–17.5	212	62	70.2	76.1	60.3	225.7	220.0
	17.5–18.5	268	67	133.4	129.2	104.1	309.2	303.7
	18.5–19.5	325	109	123.2	123.0	58.3	441.2	448.7
NGC 7044	16.5–17.5	110	18	103.1	100.7	94.4	118.8	116.3
	17.5–18.5	126	41	111.8	111.1	90.5	149.8	148.4
	18.5–19.5	135	56	118.9	115.3	86.5	173.4	180.1
	19.5–20.5	146	102	95.4	96.2	57.6	202.6	202.6
	20.5–21.5	115	87	83.8	72.2	39.6	180.9	169.0
	21.5–22.0	59	40	50.1	44.5	24.3	98.3	90.8
NGC 7510	12.0–13.0	10	1	8.6	8.6	8.6	10.0	10.0
	13.0–14.0	12	2	9.2	9.2	9.2	12.0	12.0
	14.0–15.0	12	3	4.9	4.9	4.9	12.0	12.0
	15.0–16.0	21	4	11.6	11.6	11.6	21.0	21.0
	16.0–17.0	52	5	40.1	40.1	40.1	52.0	52.0
	17.0–18.0	67	13	37.9	37.6	36.2	68.7	68.7
	18.0–19.0	74	18	34.3	34.6	31.4	77.8	79.1
	19.0–20.0	53	10	32.8	32.8	29.4	58.3	58.6
	20.0–21.0	58	11	41.4	38.2	32.0	70.6	67.6

effects of using the values of CFM or CFP for the data incompleteness correction on the slope of the MFs, and have found that the latter makes the MF slope steeper. In order to demonstrate the effects of using the values of CFM or CFB for data incompleteness correction and improper field star contamination on the LF, and hence on the slope of the cluster MF, we derived following five LFs:

$$N1 = \frac{NC}{CFBC} - \frac{NF \times AR}{CFBF},$$

$$N2 = \frac{NC}{CFMC} - \frac{NF \times AR}{CFMF},$$

$$N3 = NC - NF \times AR,$$

$$N4 = \frac{NC}{CFBC},$$

$$N5 = \frac{NC}{CFMC},$$

where *NC* and *NF* are the star counts in a magnitude bin for the cluster and field regions; (CFBC, CFMC) and (CFBF, CFMF) are the data completeness factors in the respective regions, and *AR* is the area ratio of cluster to field regions. Thus *N1* and *N2* denote the MS LFs of the cluster stars. They are corrected for the same field star contamination, but for different data incompletenesses. The distribution *N3* is the LF where star counts of cluster region are corrected for field star contamination, but not for data incompleteness, and thus represents the case where the data completeness is quite similar for both cluster and field regions. The LFs given by *N4* and *N5* are corrected only for different data incompletenesses, and thus give the combined LF of cluster and field stars. Their comparison with *N1* and *N2* can show the effect of improper field star contamination on the LFs. They are steepest in the LFs of a cluster, as field star contamination increases with decreasing brightness. A comparison of *N1* with *N2*, and of *N4* with *N5*, shows that the LFs derived using CFB and CFM as data completeness factors are almost the same. For a given star cluster, the LF denoted by *N3* is flattest, since the data incompleteness is greater for fainter stars.

4 CLUSTER MASS FUNCTION

To derive a cluster MF from the LF, knowledge of a mass–luminosity relation is required. For this, we need not only the cluster reddening, metallicity and age, but also the appropriate theoretical stellar evolutionary models. The values of reddening $E(V-I)$, distance and age used for the clusters are taken from our Papers I and II (see Table 1). The theoretical stellar evolutionary isochrones given by Bertelli et al. (1994) have been used in the present analysis. They are derived from stellar models computed with the most recent radiative opacities, and include the effects of mass-loss and convective core overshooting. The models are followed from the zero-age main sequence (ZAMS) to the central carbon ignition for massive stars and to the beginning of the thermally pulsing regime of the asymptotic giant branch phase for low- and intermediate-mass stars. As the metallicity [Fe/H] values are not known spectroscopically for any of the clusters under study, we assumed that all of them have solar metallicity and used the isochrones computed for Population I stars ($X = 0.7$, $Y = 0.28$ and $Z = 0.02$) in the present analysis.

4.1 Slope of the mass functions

To convert the LFs into MFs, we divide the numbers given in Table 5 by the mass interval, ΔM, of the magnitude bin under consideration. The value of ΔM was obtained from the mass–luminosity relations derived from the appropriate isochrones. The resulting cluster MFs in the case of the LF represented by *N1* are plotted in Fig. 5. This indicates that the MFs indeed follow a power law. The MF slope has been derived from the mass distribution, $\xi(M)$. If dN denotes the number of stars in a bin with central mass M, then the value of MF slope x is determined from the linear relation

$$\log(\mathrm{d}N) = -(1+x) \times \log(M) + \text{constant}$$

using the least-squares solution. The values of the MF slopes along with the mass range and errors are given in Table 6. The errors are formal errors resulting from the linear regression to the data points. The mass range is about $1\,M_\odot$ for all clusters except NGC 7510, where it is more than $13\,M_\odot$. This is a result of stellar evolution. As the clusters are older than 0.5 Gyr, massive stars ($\geq 2.5\,M_\odot$) have moved away from the MS and their LFs cannot be determined from the observations available in the literature. Present analysis is therefore generally limited to a relatively narrow ($\sim 1\,M_\odot$) mass range.

We derive five MF slopes, namely x_1, x_2, x_3, x_4 and x_5, from the LFs *N1*, *N2*, *N3*, *N4* and *N5* respectively. The slopes x_1 and x_2 are derived from the LFs where the same field star contamination but different data incompleteness have been applied. In the case of x_3, data incompleteness is not taken into account, while in the case of x_4 and x_5, field star contamination has not been considered. Intercomparison of these five MF slopes can throw light on the effects of using CFB or CFM for the data incompleteness correction and improper field star contamination correction on the MF slopes. They are discussed below.

4.1.1 *Effects of data incompleteness correction procedure on the MF slope*

It is worth knowing the effects of different procedures used for data incompleteness correction (see Section 3.5) on the MF slopes. Sagar & Richtler (1991) and Banks et al. (1995) have shown that

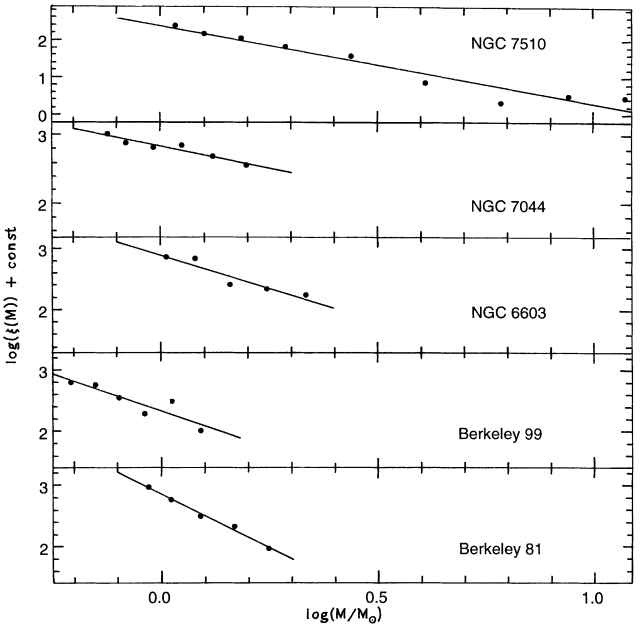

Figure 5. Plot of the mass functions, x_1, derived using Bertelli et al. (1994) isochrones. The MF is derived from the LF *N1*, which is corrected for both field star contamination and data incompleteness.

Table 6. The mass function slopes x_1, x_2, x_3, x_4 and x_5 are derived from the luminosity functions *N1*, *N2*, *N3*, *N4* and *N5* respectively for the star clusters under study. σ is the standard deviation of the slopes.

Cluster	Mass range	Mass function slopes				
	($M_\odot$)	$x_1 \pm \sigma$	$x_2 \pm \sigma$	$x_3 \pm \sigma$	$x_4 \pm \sigma$	$x_5 \pm \sigma$
Berkeley 81	0.9– 1.9	2.51±0.21	1.83±0.38	0.86±0.36	4.07±0.15	3.88±0.19
Berkeley 99	0.6– 1.4	1.43±0.58	1.55±0.60	0.95±0.66	1.67±0.28	1.71±0.28
NGC 6603	0.9– 2.4	1.14±0.44	1.13±0.38	0.24±0.52	2.27±0.22	2.28±0.23
NGC 7044	0.7– 1.7	0.30±0.20	0.10±0.23		1.13±0.13	1.04±0.20
NGC 7510	1.0–13.4	1.08±0.22	1.07±0.21	1.00±0.21	1.21±0.14	1.20±0.15

the MF slopes are on an average steeper if one uses CFP (Mateo's 1988 procedure) instead of CFM (the Sagar & Richtler 1991 procedure) for the data incompleteness correction. In order to study the effects of using CFB or CFM as the data completeness factor on the resulting MF slopes, we compare the values of x_1 with x_2 and of x_4 with x_5. In the cases of x_1 and x_4, the completeness factors (CFB) are derived from the stars recovered in both *V* and *I* images, while in the cases of x_2 and x_5 the values of CFM are determined from the minimum completeness factors of the pair. The values of x_1 and x_4 agree fairly well (within 1σ) with the values of x_2 and x_5 respectively, although the latter values are generally slightly flatter. This indicates that the MF slope does not change significantly if the values of CFM are used instead of CFB as the data completeness factor, although in principle the CFB values should be used, and this has been done in the further data analysis.

4.1.2 Effects of data incompleteness and field star contamination corrections on the MF slope

For this, one can compare the values of x_3 and x_4 with that of x_1 of a cluster. The MF slope x_3 is derived from a LF which is corrected for field star contamination but not for data incompleteness. It is the flattest for a given cluster, due to the fact that the data incompleteness is greater for fainter stars (see Table 4). The MF slope x_4 is derived from an LF which is corrected only for data incompleteness. It therefore represents the case where field star contamination is negligible. This MF slope is the steepest for a given cluster, as the field star contamination actually increases with decreasing stellar brightness. Thus we conclude that although both the corrections increase with decreasing stellar brightness, they affect the MF slope in exactly the opposite way. The MF slope becomes flatter if the data incompleteness correction is not applied, while it becomes steeper if the field star contamination correction is ignored. Except in the case of NGC 7510, for all the star clusters under study the MF slopes x_1, x_3 and x_4 differ significantly from each other, being steepest when the field star contamination is not considered and flattest when the data incompleteness is not taken into account. This shows the importance of proper correction for field star contamination and data incompleteness. It is worth mentioning here that Aparicio et al. (1993) derived a slope of 1.66 for NGC 7044. They took account of data incompleteness but, due to the lack of observations of a field region, they could not correct for field star contamination. Their value is steeper than our value, 1.13 ± 0.13, of the MF slope, x_4, which is derived in a similar way, but proper correction of both field star contamination and data incompleteness changes the value significantly and hence show their importance in the determination of MF slope of a star cluster.

In the light of the above discussion, the slope x_1 is considered as representative of the cluster MF amongst the different values of MF slope given in Table 6, since it has been derived from the LF in which both field star contamination and data incompleteness have been applied properly.

4.2 Effects of mass segregation on cluster members

In order to study the effects of mass segregation on cluster members, we divide the members into different mass groups and study their observed radial stellar surface density distribution, estimate the statistical confidence level for the difference observed between the mass groups, and analyse the variation of the average radii of the mass groups.

For the study of the spatial distribution of stars of different mass groups, we divide the cluster stars into either three or five *V*-magnitude bins, but the cluster area into a central and 2–4 annular regions, in such a way that each magnitude bin in a region generally contains a statistically significant number of cluster members. The circular area around the cluster centre is considered as the central region. The mean radii of central and annular regions are given in Table 7. For each mass group, the number density of cluster stars, ρ_i, in the *i*th zone has been evaluated as

$$\rho_i = \frac{N_i}{A_i},$$

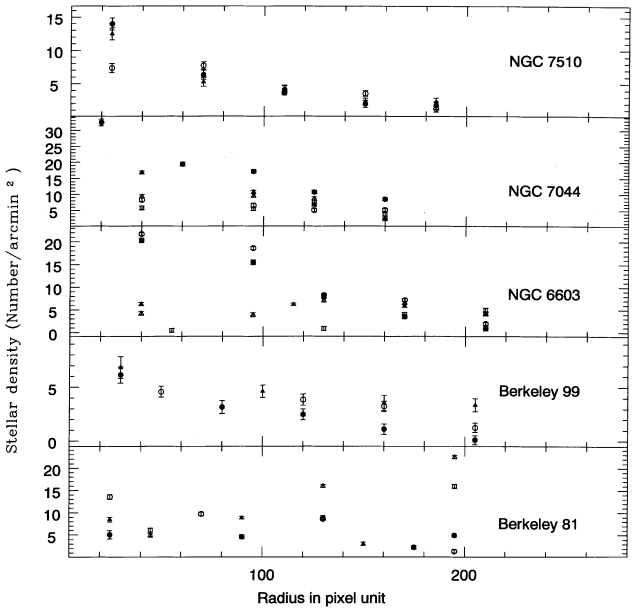

Figure 6. Radial stellar surface density distribution for stars of different mass groups. The filled circles, open circles, filled triangles, open triangles and open squares represent mass groups 1, 2, 3, 4 and 5 respectively. The lengths of the bars represent errors in the density estimation.

Table 7. The radius and stellar surface density for different mass groups of the star clusters under study. The errors in the density values are standard deviation.

Cluster	Radius range (pixel)	Stars per square arc min in the mass groups				
		1	2	3	4	5
Berkeley 81	0 – 50	5.06 ± 0.92	13.55 ± 0.54	8.45 ± 0.52		
	0 – 90				4.87 ± 0.38	6.07 ± 0.47
	50 – 90		9.70 ± 0.40			
	50 – 130	4.55 ± 0.45		8.79 ± 0.30		
	90 – 170		8.55 ± 0.28		15.98 ± 0.29	8.90 ± 0.43
	130 – 170			2.99 ± 0.35		
	130 – 220	2.23 ± 0.41				
	170 – 220		4.88 ± 0.33	1.35 ± 0.33	22.50 ± 0.32	15.91 ± 0.47
Berkeley 99	0 – 60	6.14 ± 0.74		6.84 ± 1.02		
	0 – 100		4.57 ± 0.51			
	60 – 100	3.15 ± 0.60				
	60 – 140			4.62 ± 0.58		
	100 – 140	2.46 ± 0.51	3.83 ± 0.53			
	140 – 180	1.09 ± 0.48	3.22 ± 0.48	3.55 ± 0.69		
	180 – 230	0.09 ± 0.42	1.24 ± 0.43	3.34 ± 0.59		
NGC 6603	0 – 80	20.34 ± 0.48	21.75 ± 0.31	6.30 ± 0.39	4.22 ± 0.43	
	0 – 110					0.43 ± 0.43
	80 – 110	15.48 ± 0.52	18.62 ± 0.33		3.92 ± 0.45	
	80 – 150			6.19 ± 0.28		
	110 – 150	8.13 ± 0.44	8.27 ± 0.28		7.07 ± 0.37	0.84 ± 0.46
	150 – 190	3.53 ± 0.46	7.17 ± 0.28	5.88 ± 0.32	6.56 ± 0.36	4.06 ± 0.44
	190 – 230	0.95 ± 0.53	1.94 ± 0.29	4.08 ± 0.33	4.29 ± 0.37	5.00 ± 0.43
NGC 7044	0 – 40	32.43 ± 1.00				
	0 – 80		8.27 ± 0.55	16.85 ± 0.48	9.36 ± 0.55	5.78 ± 0.62
	40 – 80	19.42 ± 0.62				
	80 – 110	17.16 ± 0.57	6.58 ± 0.60	10.73 ± 0.53	9.61 ± 0.58	5.53 ± 0.60
	110 – 140	10.71 ± 0.53	5.09 ± 0.54	6.81 ± 0.50	8.67 ± 0.52	7.49 ± 0.57
	140 – 180	8.49 ± 0.45	5.17 ± 0.41	2.26 ± 0.46	2.68 ± 0.49	3.78 ± 0.52
NGC 7510	0 – 50	13.98 ± 0.92	7.37 ± 0.70	12.48 ± 0.89		
	50 – 90	6.35 ± 0.68	7.74 ± 0.54	5.28 ± 0.68		
	90 – 130	4.08 ± 0.58	3.76 ± 0.47	4.23 ± 0.57		
	130 – 170	1.97 ± 0.53	3.53 ± 0.41	2.33 ± 0.52		
	170 – 200	1.72 ± 0.57	1.20 ± 0.46	2.32 ± 0.54		

where N_i is the number of cluster stars, and A_i is the area of the zone considered. To get the value of N_i, data incompleteness and field star contamination corrections have been applied to the observed number of star, N_o, using the relation

$$N_i = \frac{N_o}{CFBC} - NF,$$

where CFBC is the completeness factor for the considered MS brightness in the $V, (V-I)$ diagram. The value of NF, the field star contamination, for the area A_i, has been derived from the observed number of stars in the field region, after applying the appropriate corrections for the data incompleteness and area difference between the considered cluster and field regions. The stellar surface density derived in this way for all the clusters is given in Table 7 along with the errors. The stellar surface density (ρ) versus radius (R) plots for all mass groups of the clusters under discussion are given in Fig. 6. This shows that the radial stellar surface density distribution differs from one mass group to another in each cluster except NGC 7510.

It seems that

$$\log \rho = a + b \log R,$$

where a and b are the unknown coefficients. In each observed stellar density profile of a cluster, the above relation is fitted and coefficients are estimated using the least-squares solution. The slope b, with its standard derivation, and the absolute value of correlation coefficient r are given in Table 8. As the value of r is generally greater than 0.7, the assumption of the above linear relation for the plots in Fig. 6 may be justified. A similar power law has also been observed by Sellgren (1983) and Sagar et al. (1988) for some other open clusters. The value of b is plotted against the average mass of the group in Fig. 7. This shows that, except for NGC 7510, in all clusters the value of b varies with mass of the group, indicating clearly the presence of mass segregation. We assume a normal error distribution for deriving the statistical significance level of the differences between the slopes of different mass groups of a cluster. In NGC 7510, the values of b for all the mass groups are quite similar. The values of b in Berkeley 81 fall into two groups. The b-values of the three most massive mass groups agree within errors; their weighted average is -0.45 ± 0.11. The average value of the two least massive mass groups is 1.02 ± 0.06, and it differs from that of massive group at a 11σ level. In Berkeley 99 and NGC 6603, the maximum value of b is for the lowest mass group, and as the average mass of the group increases the value of b decreases. The values of b for the least and most massive mass groups of Berkeley 99 and NGC 6603 differ at 1.8 and 4.2σ levels respectively. In the case of NGC 7044, the maximum value of b is for the least massive group. It has maximum difference with the b-value of mass group 3. The difference is significant at a 1.9σ level. These analyses indicate

Table 8. The cluster age (T) in years, dynamical relaxation time (T_e) in years and the observed radial stellar surface density slope (b) for different mass groups of the clusters under study. The standard deviation of the slope is denoted by σ_b. The absolute value of the linear correlation coefficient is r. The average radius (R_a) of a mass group is in terms of the cluster radius.

Cluster	$\log(T_e)$	log(T)	Mass group	Range in V (mag)	Range in Mass ($M_\odot$)	R_a	$b \pm \sigma_b$	r
Berkeley 81	7.9	9.0	1	16.0−18.0	2.06−1.61	0.52	−0.37±0.25	0.83
			2	18.0−20.0	1.61−1.14	0.53	−0.44±0.13	0.92
			3	20.0−21.0	1.14−0.97	0.45	−0.78±0.42	0.80
			4	21.0−22.0	0.97−0.84	0.69	1.05±0.06	0.99
			5	22.0−23.0	0.84−0.74	0.67	0.60±0.22	0.94
Berkeley 99	8.1	9.5	1	16.5−19.0	1.43−1.06	0.40	−1.76±0.76	0.80
			2	19.0−21.0	1.06−0.80	0.53	−0.73±0.44	0.77
			3	21.0−23.0	0.80−0.62	0.59	−0.39±0.03	0.99
NGC 6603	7.7	8.7	1	12.0−16.0	2.78−1.76	0.42	−1.63±0.58	0.85
			2	16.0−18.0	1.76−1.20	0.44	−1.25±0.47	0.84
			3	18.0−19.0	1.20−1.03	0.59	−0.18±0.15	0.66
			4	19.0−20.0	1.03−0.89	0.62	0.16±0.23	0.37
			5	20.0−21.0	0.89−0.77	0.79	1.88±0.59	0.91
NGC 7044	7.7	9.2	1	15.0−18.0	1.80−1.32	0.55	−0.61±0.11	0.96
			2	18.0−19.0	1.32−1.12	0.59	−0.37±0.07	0.96
			3	19.0−20.0	1.12−0.97	0.47	−1.24±0.51	0.86
			4	20.0−21.0	0.97−0.84	0.54	−0.62±0.57	0.61
			5	21.0−22.0	0.84−0.73	0.61	−0.13±0.31	0.29
NGC 7510	7.4	7.0	1	12.0−17.0	13.41−2.28	0.48	−1.07±0.13	0.98
			2	17.0−19.0	2.28−1.39	0.53	−0.75±0.34	0.79
			3	19.0−21.0	1.39−0.99	0.52	−0.86±0.08	0.99

a high level of statistical confidence (>90 per cent) in the observed mass segregation in Berkeley 81, Berkeley 91, NGC 6603 and NGC 7044.

We list in Table 8 estimated average radii for the different mass groups of a cluster. The radii for the low-mass stars are larger by a factor of 1.3 to 1.9 than those of high-mass stars, except in the case of NGC 7510. This again indicates more central concentration of high-mass stars in comparison to low-mass stars for Berkeley 81, Berkeley 99, NGC 6603 and NGC 7044.

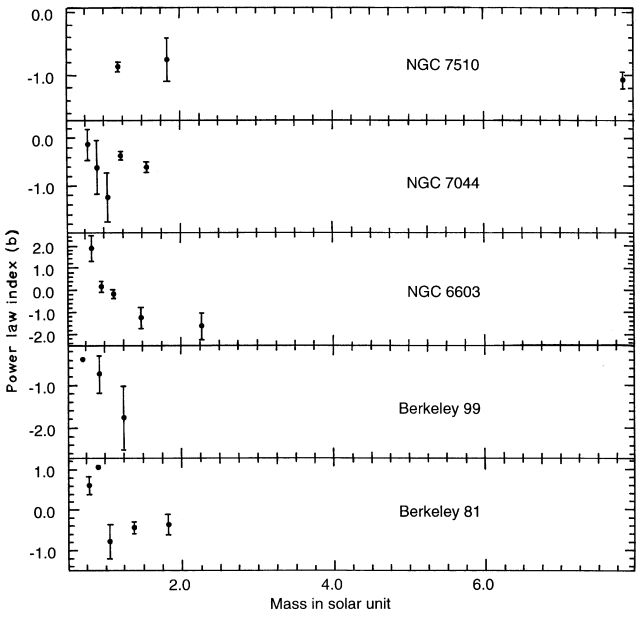

Figure 7. The plot of the MF slope versus the average mass of the group. The length of each bar represents the least-squares error in the MF slope of the mass group.

4.3 Effects of the field region being close to the cluster on the MF slope

The MF slopes of a cluster given in Table 6 are derived from counts of those stars which are located within a radial distance of R from the cluster centre. These star counts are corrected for the field star contamination, which is determined from a region located not very far from the cluster region (see Table 2). It would be useful to know

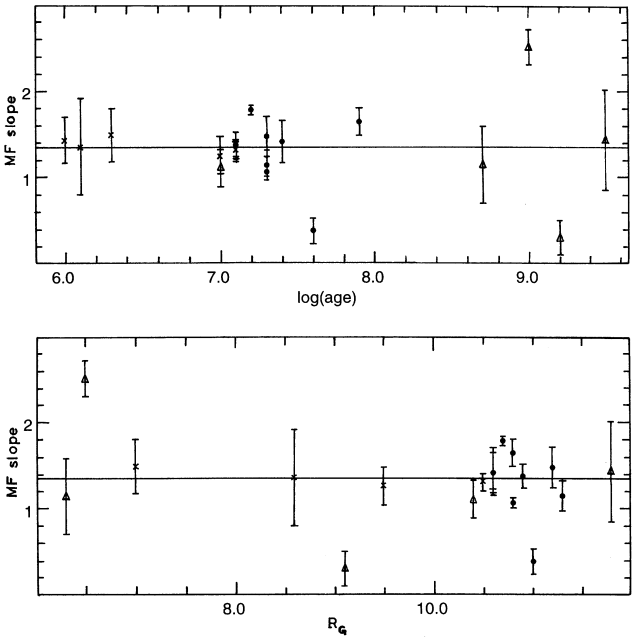

Figure 8. Dependence of the MF slope on the Galactocentric distance, R_G and age of the star cluster. Data taken from Phelps & Janes (1993), Sagar et al. (1986) and present work are denoted by ●, × and △ respectively. The horizontal lines represent the value of Salpeter slope.

the change in the present MF slopes, if the cluster regions were extended well beyond its radius and the field star contamination were determined from a region located far away from the cluster centre so that all cluster members are included in the cluster region but none of them are located in the field region. We do not expect any change in the MF slope of NGC 7510, as mass segregation is not present in the cluster. However, the MF slopes of all other clusters under study may be affected due to the presence of mass segregation effects in them. The larger area for the cluster region would steepen the MF slope, as the high-mass stars are more concentrated towards the cluster centre than the low-mass stars due to presence of mass segregation. On the other hand, a possible over-correction for field star contamination due to relatively nearby location of the field region from the cluster would flatten the presently derived MF slope since, due to the presence of mass segregation, relatively more low-mass stars would be subtracted than the high-mass cluster members. The present MF slope for the clusters under discussion may therefore not be very different from the actual one.

5 DYNAMICAL STATE OF THE CLUSTERS

Before deriving conclusions from the studies described in the last section, it is necessary to know whether the location of stars in these clusters is representative of primordial (resulting from the processes of star formation) or not. At the time of formation, if the cluster had a uniform spatial stellar mass distribution, then as the cluster evolves dynamically, the spatial stellar mass distribution changes and we would find the massive stars concentrated towards the centre of the cluster, as the low-mass stars attained high velocity and moved away from the cluster centre. While theory and simulations show that complete energy equipartation is unlikely to be established in a star cluster (Spitzer 1969; Inagaki & Saslaw 1985; Meylan & Heggie 1997, and references therein), mass segregation certainly does develop in the time-scale, $t_{\rm eg}$, required to exchange energy between stars of different mass by small angle scattering. If all of the stars in a cluster begin with the same spatial distribution, stars of mass m_1 will at least initially have $t_{\rm eg,1} = (< m > /m_1)t_{\rm r}$, where $t_{\rm r}$ is the local two-body relaxation time at radius r (Spitzer 1969). Thus mass segregation will be most rapid for the most massive stars at the smallest radii where $t_{\rm r}$ is shortest. Numerical simulations with a range of stellar masses (e.g. Inagaki & Saslaw 1985; Chernoff & Weinberg 1990) do show the profiles of the heaviest stars changing most rapidly, and the effects of mass segregation propagating outward through the cluster. The simulations show that significant mass segregation among the heaviest stars in the core occurs in the local relaxation time, but affecting a large fraction of the mass of the cluster requires a time comparable to the average relaxation time averaged over the inner half of the mass. The dynamical relaxation time, $T_{\rm e}$, is the time in which the individual stars exchange energies and their velocity distribution approaches a maxwellian equilibrium. It is given by

$$T_{\rm e} = 8.9 \times \frac{R_{\rm h}^2 \sqrt{N}}{\log(0.4N)\sqrt{< m >}},$$

where N is the number of cluster members, $R_{\rm h}$ is the radius containing half of the cluster mass and $< m >$ is the average mass of the cluster stars (cf. Spitzer & Hart 1971). Due to our inability of estimating $R_{\rm h}$ from the present data, we assume that $R_{\rm h}$ is equal to half of the cluster radius listed in Table 2. These angular values are converted into linear values by taking the cluster distances listed in Table 1. The average mass $< m >$ and the value of N are based on the cluster stars used in the present analysis. The values of $T_{\rm e}$ estimated in this way for each cluster are given in Table 8. The data considered for this work is limited up to certain brightness. Inclusion of cluster members fainter than the limiting V magnitude will decrease the value of $< m >$ and increase the value of N. This will result higher values of $T_{\rm e}$. Hence the value of $T_{\rm e}$ given in Table 8 may be considered as the lower limit of $T_{\rm e}$.

A comparison of cluster age with its dynamical relaxation time (see Table 8) indicates that the former is always greater than the latter, except for NGC 7510. Thus one may conclude that dynamical evolution has produced observed mass segregation in the clusters under study. In contrast, primordial mass segregation has been observed in some young star clusters of our Galaxy (Sagar et al. 1988; Raboud & Mermilliod 1998) as well as of the Magellanic Clouds (Subramaniam, Sagar & Bhatt 1993; Fischer et al. 1998, and references therein).

6 DISCUSSION OF THE MASS FUNCTION SLOPES

In this section we compare the MFs of the programme star clusters with each other, as well as with the similar previous studies of Galactic open clusters. In the light of the discussion in Section 4, amongst the different values of x given in Table 6, the slope of x_1 is considered as representative of the cluster MF.

6.1 Comparison of the MFs of the star clusters under study

The MF slope for the youngest cluster NGC 7510 is based on a wide range of mass, while for others it is derived from a relatively narrow mass range. The MF slopes for Berkeley 91, NGC 6603 and NGC 7510 are not very different from the Salpeter (1955) value of 1.35. However, the slope is significantly steeper for Berkeley 81 but flatter for NGC 7044 in comparison to the Salpeter value. For these two star clusters, the value of the MF slope depends strongly upon the procedure used for data incompleteness and field star contamination correction (see Table 6). In order to establish firmly the departure of these MF slopes from the Salpeter value, further observations and studies are required, as both clusters are old and dynamically evolved. As the high-mass stars are more concentrated towards cluster centre than the low-mass stars in the presence of radial mass segregation, the true IMF may be steeper than the derived MF slope, and hence it may be considered as an upper limit. At present, the actual value of IMF cannot be derived, as we are unable to correct the observed MF slope for the effects of dynamical evolution.

Unfortunately, the structural and kinematical parameters of the clusters under discussion are presently unknown. It would be interesting to investigate their relations with the MF slope of the clusters, once they become known.

6.2 Dependence of the MF slope on $R_{\rm G}$ and age of the open star cluster

The present MF determinations, along with the previous reliable estimates of MF slope given by Sagar et al. (1986) and Phelps & Janes (1993) for individual objects, have been used to study the dependence of the MF slope on the Galactocentric distance, $R_{\rm G}$, and age of the star cluster. The distance and age of these objects are taken from their respective studies. In converting geocentric distance to Galactocentric distance, the distance between the Sun and

the Galactic Centre is taken as 8.8 kpc. Fig. 8 shows the plot of MF slope versus R_G and cluster age. The range in R_G is from 6 to 12 kpc, while the ages of the clusters range from 1 to 3200 Myr. The value of the Salpeter (1955) slope is shown as a straight line in Fig. 8. The values of x seem to have no dependence on either R_G or cluster age and all are close to the Salpeter value, except for a few random discrepant values for which dynamical evolution rather than intrinsic difference in the IMF of these clusters seems to be responsible, as most of them are old. However, more observations are needed to confirm these findings and also to understand the effects of dynamical evolution on the IMF slope.

7 SUMMARY AND CONCLUSIONS

We have calculated luminosity and mass functions for five distant star clusters using CCD *BVI* data. Except for NGC 7510, whose age is ~10 Myr, all are older than 0.5 Gyr. The completeness of the present CCD data has been determined empirically as a function of MS brightness for both the cluster and the field regions. The observed cluster LF has been corrected for both data incompleteness and field star contamination. We have used theoretical stellar evolutionary isochrones for converting the true LFs into MFs. The dynamical evolutionary effects might have already affected the IMF of the star clusters under study except for NGC 7510, as they are older than 100 Myr, which is a typical time-scale for dynamics to affect such stellar systems. The main conclusions of this study are as follows.

(1) Improper corrections for field star contamination and data incompleteness can yield quite different value for the MF slope. Although both corrections increase with decreasing brightness, they affect the MF slopes in exactly the opposite way. The MF slope becomes flatter if a data incompleteness correction is not applied, while it becomes steeper if a correction for field star contamination is ignored.

(2) The present-day MF of NGC 7510 can be assumed to be equivalent to the IMF, since the dynamical relaxation time is longer than its age (see Table 8). The MF of this cluster has a slope similar to Salpeter's slope of IMF in the solar neighbourhood.

(3) In the mass range of 0.6 to 2 $M_\odot$, the MF slopes of the four intermediate age and old star clusters differ significantly from each other. They range from 0.3 to 2.5. The MF slopes 1.4 ± 0.6 and 1.1 ± 0.4 for Berkeley 99 and NGC 6603 respectively agree within the errors with each other, but differ significantly from the slope 2.5 ± 0.2 for Berkeley 81 and 0.3 ± 0.2 for NGC 7044. We therefore conclude that the MF *does* vary among the clusters under study.

(4) There are radial variations in the MF slopes of all the four intermediate-age and old star clusters. As the dynamical relaxation times are shorter than the ages of these clusters (see Table 8), the dynamical evolution seems to be responsible for the observed radial mass segregation in them. On the other hand, primordial mass segregation has been observed in a number of young star clusters of our Galaxy as well as of the Magellanic Clouds. It is therefore important to understand the physical processes of star formation responsible for producing primordial mass segregation, and it is not observed in all young star clusters.

(5) The value of MF slope seems to not depend on either R_G or cluster age except for some dynamically evolved older star clusters whose MF slopes differ significantly from others. Further studies are needed to determine whether the dynamical evolution results in differences in the structural and kinematical parameters of the clusters, or whether the intrinsic differences in their IMF are responsible for the observed differences in their MF slopes.

ACKNOWLEDGMENTS

The valuable comments given by the referee M. Mateo improved the scientific content of the paper significantly. We thank Vijay Mohan and A. K. Pandey for critical reading of the manuscript, and the PATT for the allotment of observing time for this project. This work is based on observations obtained on the Isaac Newton Telescope (INT), La Palma Observatory.

REFERENCES

Aparicio A., Alfaro E. J., Delgado A. J., Rodriguez-Ulloa J. A., Cabrera-Caño J., 1993, AJ, 106, 1547
Banks T., 1994, PhD thesis, Victoria University of Wellington, New Zealand
Banks T., Dodd R. J., Sullivan D. J., 1995, MNRAS, 274, 1225
Bertelli G., Bressan A., Chiosi C., Fagotto F., Nasi E., 1994, A&AS, 106, 275
Bertelli G., Bressan A., Chiosi C., Ng Y. K., Ortolani S., 1995, A&A, 301, 381
Chernoff D. F., Weinberg M. D., 1990, ApJ, 351, 121
Fischer P., Pryor C., Murray S., Mateo M., Richtler T., 1998, AJ, 115, 592
Inagaki S., Saslaw W. C., 1985, ApJ, 292, 339
King I. R., 1962, AJ, 67, 471
Kjeldsen H., Frandsen S., 1991, A&AS, 87, 119
Landolt A. V., 1983, AJ, 88, 439
Lyngå G., 1987, Catalogue of Open Cluster Data, 5th edn. Centre de Donnees Stellaires, Strasbourg, France, 1/1 S 7041
Mateo M., 1988, ApJ, 331, 261
Mateo M., 1993, in Smith G. H., Brodie J. P., eds, ASP Conf. Ser. Vol. 48, The Gobular Cluster–Galaxy Connection. Astron. Soc. Pac., San Francisco, p. 387
Meylan G., Heggie D. C., 1997, A&AR, 8, 1
Phelps R. L., Janes K. A., 1993, AJ, 106, 1870
Piskunov A. E., 1976, Nauch. Inf., 22, 47
Raboud D., Mermilliod J.-C., 1998, A&A, 329, 101
Richtler T., 1994, A&A, 287, 517
Sagar R., 1987, MNRAS, 228, 483
Sagar R., Griffiths W. K., 1991, MNRAS, 250, 683 (Paper I)
Sagar R., Griffiths W. K., 1998, MNRAS, 299, 1 (Paper II)
Sagar R., Richtler T., 1991, A&A, 250, 324
Sagar R., Piskunov A. E., Myakutin V. I., Joshi U. C., 1986, MNRAS, 220, 383
Sagar R., Myakutin V. I., Piskunov A. E., Dluzhnevskaya O. B., 1988, MNRAS, 234, 831
Salpeter E. E., 1955, ApJ, 121, 161
Sellgren K., 1983, AJ, 88, 985
Scalo J. M., 1986, Fundam. Cosmic Phys., 11, 1
Scalo J. M., 1998, in Gilmore G., Parry I., Ryan S., eds, The Stellar Initial Mass Function. Proceedings of the 38th Herstmonceux Meeting, in press
Spitzer L., 1969, ApJ, 158, L139
Spitzer L., Hart M. H., 1971, ApJ, 164, 399
Stetson P. B., 1987, PASP, 99, 191
Stetson P. B., 1991, in Janes K. A., ed., ASP Conf. Ser. Vol. 13, The Formation and Evolution of Star Clusters. Astron. Soc. Pac., San Francisco, p. 88
Subramaniam A., Sagar R., Bhatt H. C., 1993, A&A, 273, 100
van den Bergh S., Sher D., 1960, Publ. David Dunlop Obs., 2, 203